ICOOL Simulation of 10-20 GeV FFAG with Quasi-Realistic End Fields

J.S.Berg, R.Fernow, S.Kahn, R.B.Palmer, D.Trbojevic

DRAFT 3/8/2003

Contents

1 Introduction

Non-Scaling FFAGs were first proposed by Carol Johnstone[1]. It was shown that a strongly focusing FODO ring could be designed with a momentum acceptance covering up to a factor of 3. Dejan Trbojevic[2] introduced a triplet design that appears to be more isochronous and has smaller circumference and apertures. This paper will present simulations done on a design from Dejan.

Most simulations of such FFAGs have been done using idealized hard edged magnetic fields and varying approximations to higher order effects. Only the study by Meot[3] included an approximation to the end fields, but even here the end fields used were required not to overlap with any neighboring magnet. At least in the case studied, this would be a poor approximation. This study, using ICOOL[4] allows end fields to overlap. It does this by determining the fields along the beam axis using hyperbolic tangent expressions for the end fields, allowing overlap. These axial fields are then Fourier analyzed and the fields at all locations derived from these Fourier components.

2 Input parameters

The study is based on a lattice proposed by Dejan Trbojevic with the following parameters

	Len m	B_o T	G_o T/m
gap	1.0328		
1	.5	-3.4099	66.978
gap	.1672		
2	1.5	5.814	-35.701
gap	.1672		
3	.5	-3.4099	66.978
gap	1.0328		

Parameters of magnets as provided by Trbojevic

These parameters describe fields assumed to stop abruptly at the magnet ends, and will not contain some non-linear effects that any real magnet will have. In addition, realistic ends will significantly change the focusing properties of the magnets.

However, since this non- Maxwellian assumption has been used in other simulations, and ICOOL can use this assumption, we first simulate it with ICOOL so that comparisons can be made with these other codes.

To give a more realistic drop off of the magnets, we will use the following hyperbolic tangent form.. More sophisticated end fields can easily be tried later.

$$B \;=\; B_o \,\frac{B_{\rm fac}}{2}\,\left(\frac{e^{(z-z_1)/\Gamma_B}-e^{-(z-z_1)/\Gamma_B}}{e^{(z-z_1)/\Gamma_B}+e^{-(z-z_1)/\Gamma_B}} \;-\; \frac{e^{(z-z_2)/\Gamma_B}-e^{-(z-z_2)/\Gamma_B}}{e^{(z-z_2)/\Gamma_B}+e^{-(z-z_2)/\Gamma_B}}\right)$$

where z_1 is the z position of the magnet start and z_2 is the position of the magnet end.

A similar expression is used for the field gradient G, but in this, the fall off parameter Γ_G has a value a factor of two smaller.

$$\Gamma_G \;=\; \frac{\Gamma_B}{2}$$

The faster fall off for the gradients reflects the faster theoretical power fall off of a quad vs a dipole. The factors B_{fac} were chosen to give performance similar, but not identical to the hard edged case. The factors, and resulting maximum fields, used are given below. The Fields are plotted in fig 1.

	Len m	Bfac	Gfac	Γ_B m	$B_{\rm max}$ T	$G_{\rm max}$ T/m
gap	1.0328					
1	.5	1.2	1	.2	-3.36	66.03
gap	.1672					
2	1.5	1.02	1	.2	5.92	-35.70
gap	.1672					
3	.5	1.2	1	.2	-3.36	66.03
gap	1.0328					

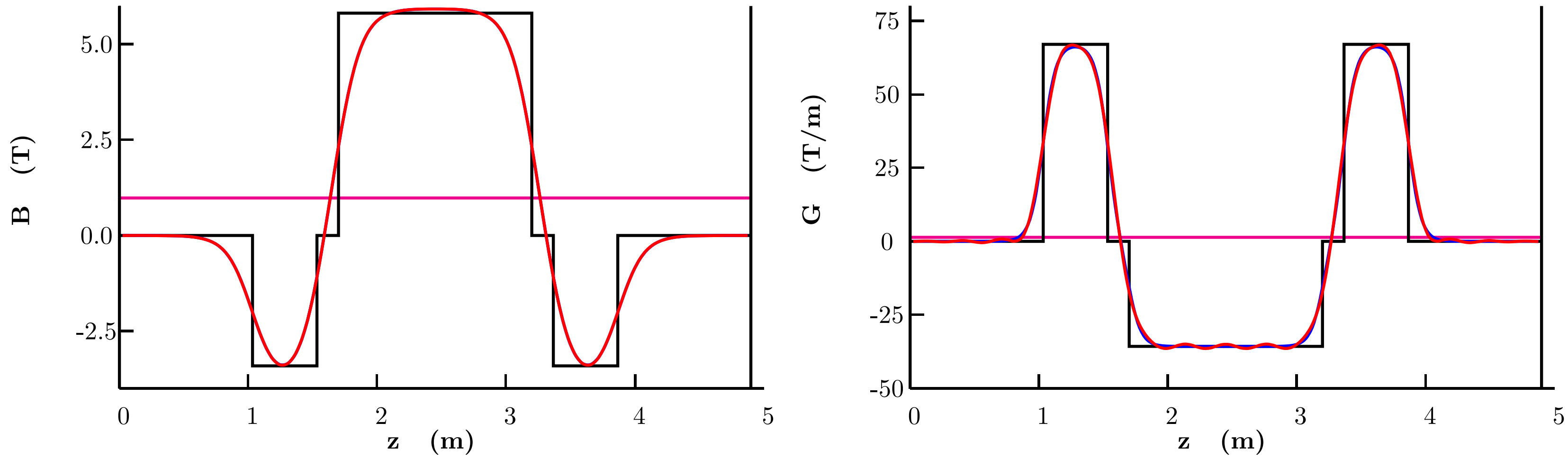

Figure 1: Shapes of a)hard endged fields (black), b) fields including htan end fields (blue), c) fields reproduced from 15 Fourier components (red).

Modified parameters including end fields

The mean bending per cell is not quite the same in the two cases, so the number of cells and circumferences are a little different:

		hard ends	htan ends
cell	m	4.9	4.9
n cells		59	65
circ	m	289	318

parameters for each example

The field strengths as a function of length were Fourier analysed, yielding the following coefficients. Sextupole terms due to the z variation of the quadrupoles will be derived by ICOOL. Sextupole terms due to the coil end shapes can be added when available.

i	B(i) T	G(i) T/m
0	.9803195	2.740101
1	-2.895885	16.53893
2	2.979532	-34.93562
3	-.5018952	6.650915
4	-1.210014	20.89505
5	.6177055	-9.08317
6	.1855154	-8.069601
7	-.1763015	4.489265
8	4.405256E-02	1.35215
9	-3.883789E-02	.1640327
10	-1.388343E-02	.458303
11	4.675247E-02	-1.96029
12	-7.055193E-03	-.5571176
13	-1.463328E-02	1.725461
14	1.062646E-03	.5901405
15	1.972909E-03	-1.068816

Fourier components of bnding and gradient fields

The Fields and Gradients vs z for the hard edged example, the soft end example with htan fall offs, and the fields from the Fourier approximation are shown in Fig1

3 ICOOL Simulation

Tracks were traced through a number of identical cells, in which the fields were derived from the axial fields and gradients given by the above Fourier approximation. One inital track per momentum was introduced at the midpoint of the long drift where rf would be placed.

The tracks are started on the determined closed orbit for that momentum, and, for this initial study, given small initial angles (corresponding to 3 Pi mm), with equal angles in the x and y planes. In each case the track positions were observed after each full cell, plotted on a phase dpot and fitted to ellipses (yellow ellipses indicate a poor fit from which data will not be used. 11 Momenta were tracked in steps of 1 GeV/c from 10 to 20 GeV/c. In fig.2 the phase plots and fitted ellipses are shown.

The same proceedure was followed using the hard edged initial design.

In fig.3 the closed orbit displacements, fitted beta functions, tunes, and closed orbit offsets are shown for both the hard edged and quasi-realistic cases.

The ICOOL data files are given in the appendix.

4 Required apertures and peak fields

A second ICOOL run was made with output at several positions along each cell. For this run, three initial tracks were introduced: a) with amplitude in x, b) the same amplitude in y, and $1/\sqrt{2}$ of these amplitudes in both x and y simultaneously. The amplitudes corresponded to the required 30 pi mm acceptance.

The track positions are plotted in fig.4 at the centers of the rf and magnets, and at the end of the longer defocus combined function magnet, together with both circles an ellipses that contain all tracks. A second circle or ellipse indicates a plausible coil inside dimension, assuming that a 30% aperture increment is needed to assure adequate field quality.

The tracks startrd with no y component (blue) remain in the mid plane as expected. Those with

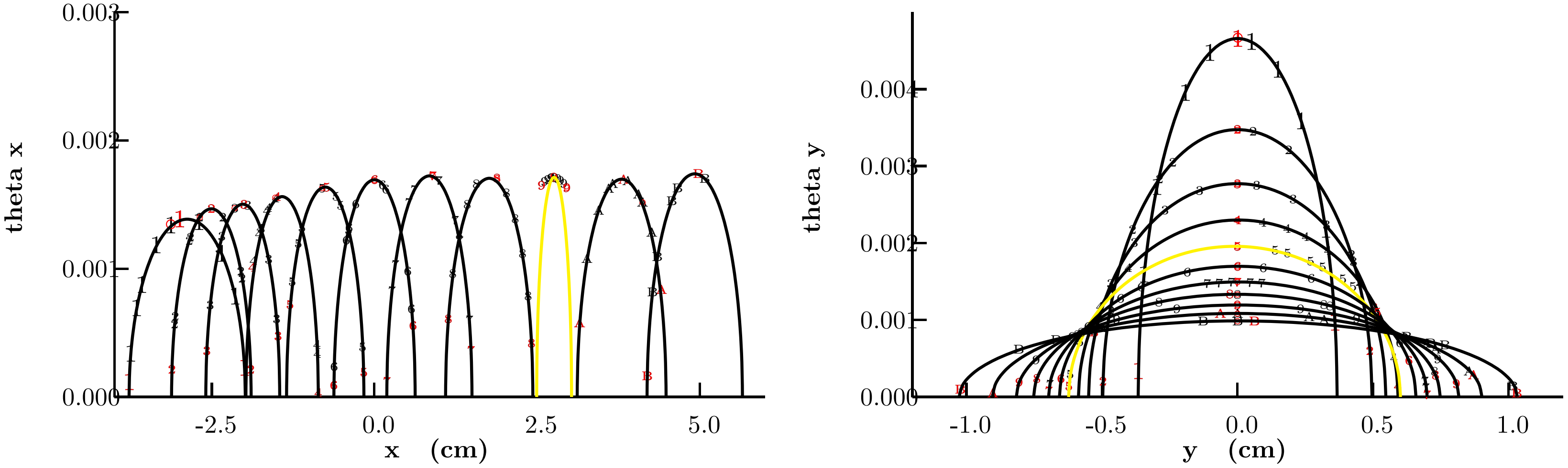

Figure 2: For htan ends: ICOOL phase plots at ends of 20 cells, from small amplitude (emittance=3 pi mm) tracks, injected with equal amplitudes in both x and y, with momenta in 1 GeV steps from 10 to 20 GeV. Fitted ellipses are shown as used to derive tunes, betas and orbit length. A yellow ellipse indicates a poor fit for which the data will not be used

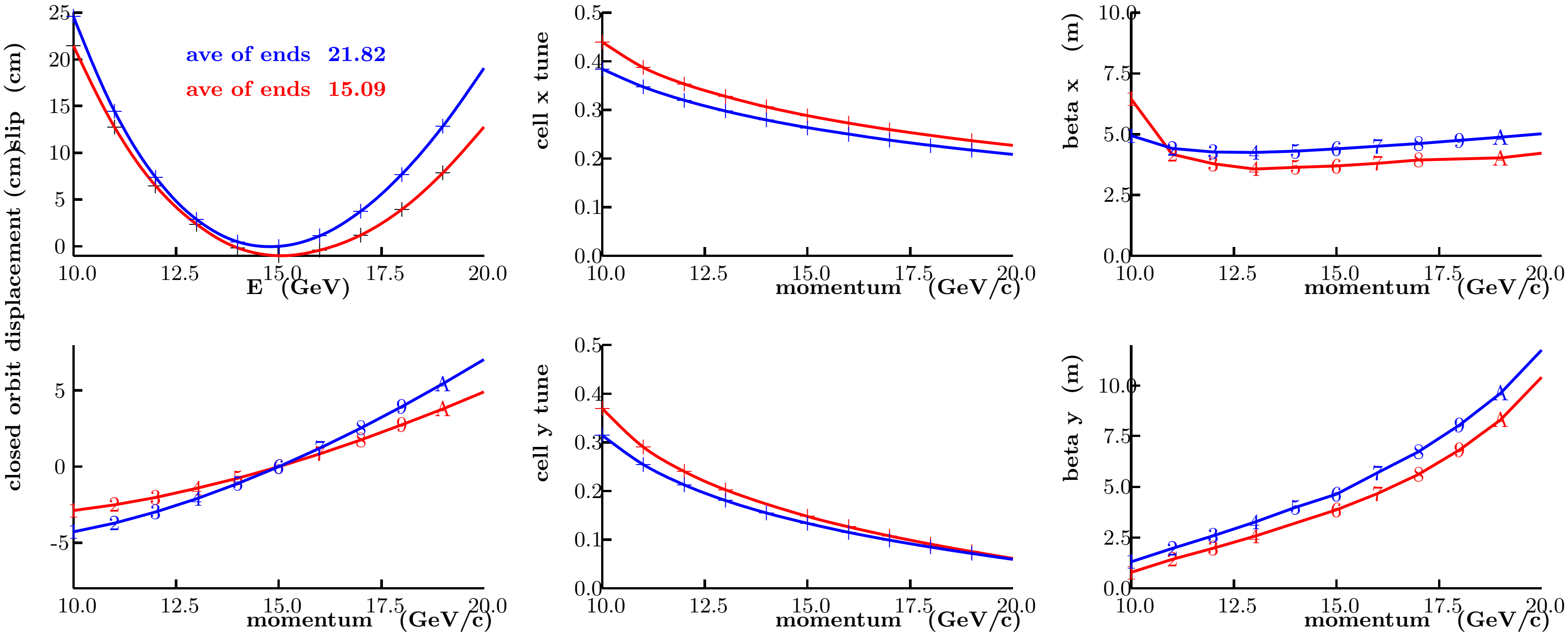

Figure 3: Parameters as a function of momentum for hard edged example (blue) and htan edged example (red): a) differences in orbit per revolution, b) x tune per cell, c) beta x at center of rf, d) closed orbit displacement at center of rf, e) y tune per cell, f) beta y at center of rf straight.

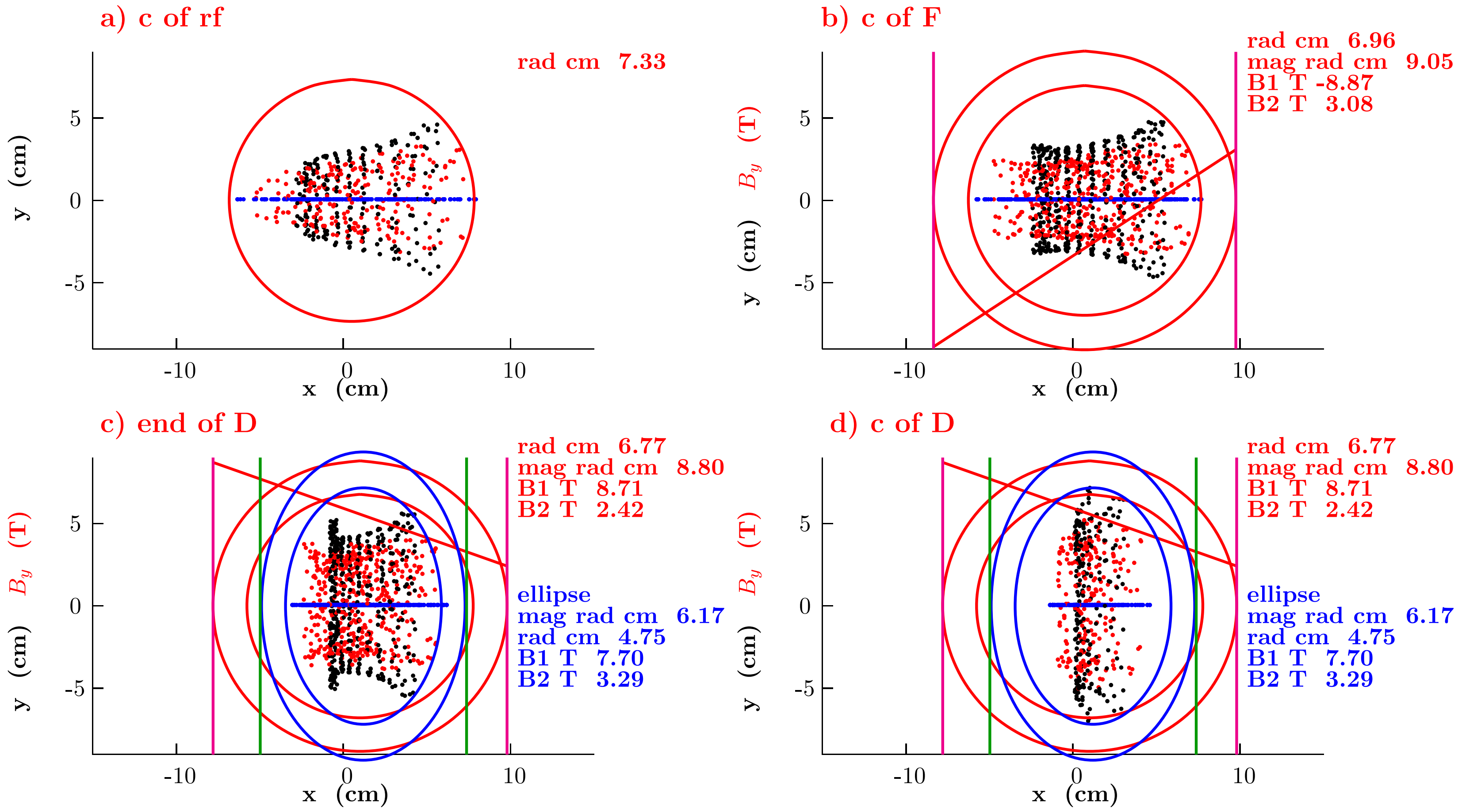

Figure 4: Magnetic fields vs x and track positions in x vs.y over 50 cells in a) center of rf straight, b)center of focus combined function magnet, c) end of defocus combined function magnet, d)center of defocus combined function magnet.

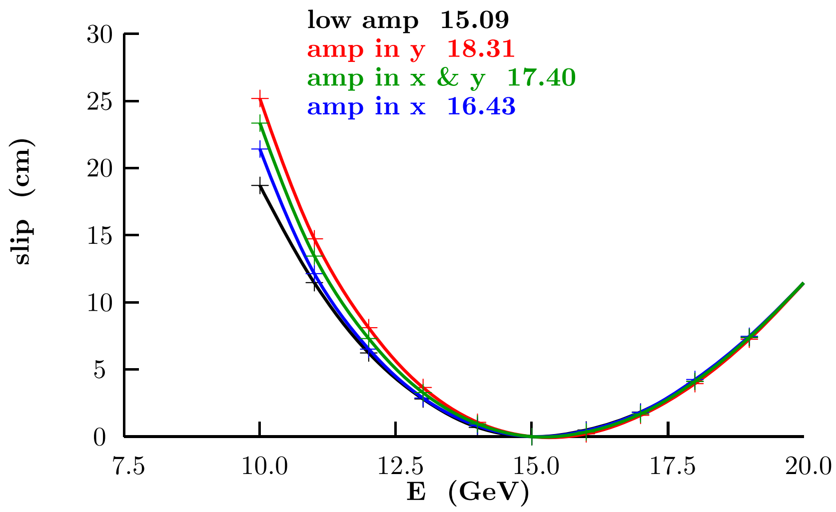

Figure 5: Differences in orbits around ring for a) low amplitudes; b) 30 pi mm in y; c) 30 pi mm in x&y; d) 30 pi mm in x. The numbers given are averages of the max and min energies in cm.

amplitudes in x and y paint a rectangular pattern. Those injected with only amplitude in the y direction remain mostly in that plane, but do have some significant coupling as seen by a widening of the patterns.

The peak field of the defocus combined function magnet would be about 1 T less (7.7 vs 8.7 T) if the magnets were shaped as vertical ellipses. This could make a significant difference in cost since it may allow 4.2 deg and NiTi conductor, instead of 2 deg or NbSn.

5 Amplitude effect on phase slip

Fig.5 shows that there is a significant increase in the orbit lengths for large amplitude tracks at low momenta, but a negligible effect at high momenta. The effect is greater for motion in the y direction.

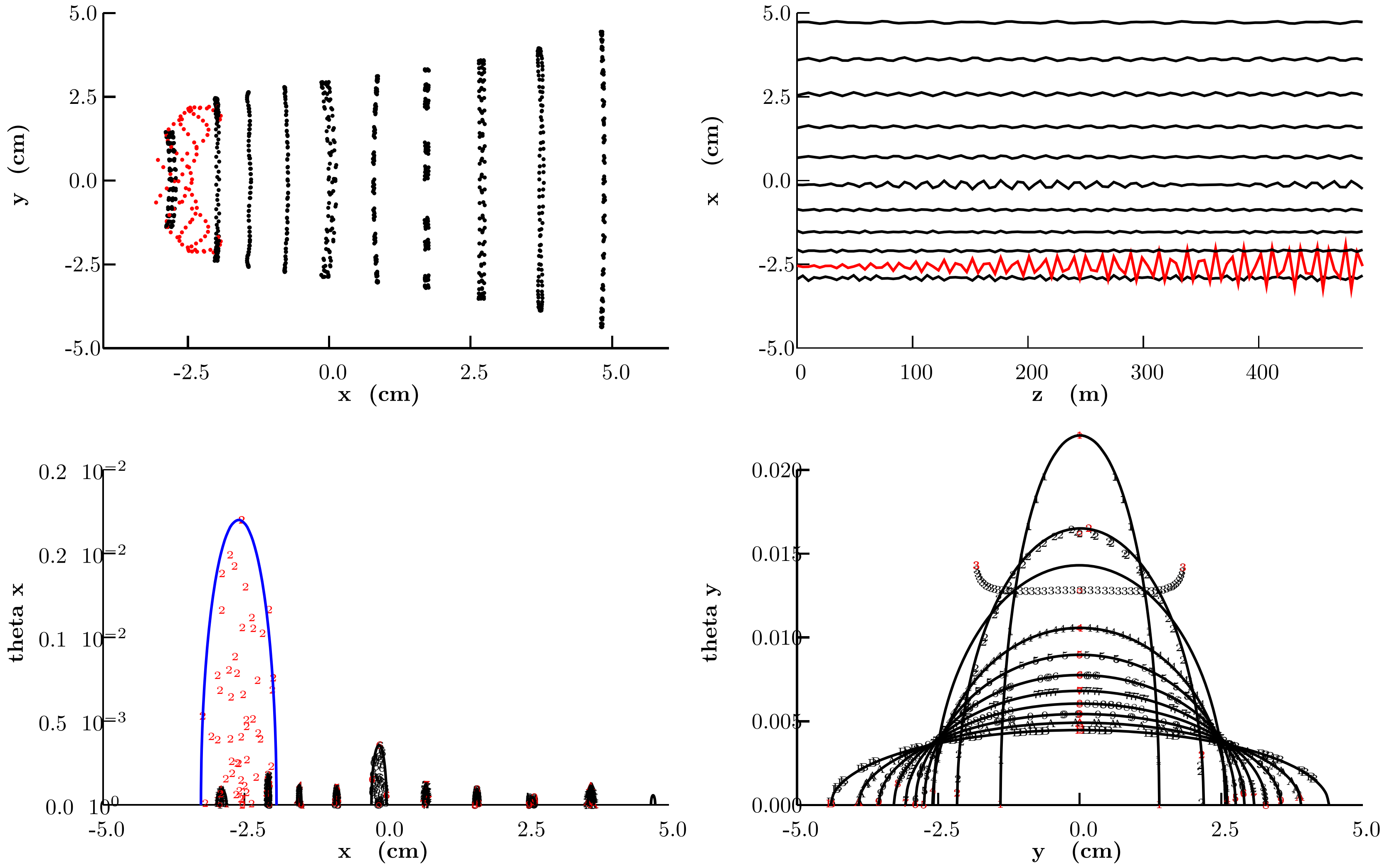

Figure 6: plots of motions at the center of the rf, with of particles with 10 momenta (9.85 to 19.85 GeV in steps of 1 GeV), injected with large amplitude (30 pi mm), only in the y plane, tracked through 100 cells: a) x y positions at the center of the rf straights, b) x positions vs z, c) phase plots in the x direction, d) phase plots in the y direction.

6 Non-linear resonances

In order to study non-linear effects, ICOOL was run separately with a 30 pi mm inital angle in y, but no amplitude in x. As before, runs were made with 11 iniial momenta, spaced by 1 GeV/c, but, to search for resonances, the initial momenta were stepped by 0.1 GeV/c steps. Resonant effects were most apparent with an inital momentum of 9.85 GeV/c. Results from this run are shown in fig.6.

Three different non-linear effects were observed.

6.1 Half integer resonance

Instability at 30 pi mm, is observed when the momentum is equal or lower than 9.6 GeV/c. This is due to the approach to the half integer tune.

6.2 x-y Mixing

Such effects have already been reported by Meot[3].

Fig. 6a shows the $x - y$ positions at the end of each cell for 50 cells. It shows primarily vertical bands corresponding to the expected y motion, but in one case (10.85 GeV) the motion is seen to be greatly broadened in the x direction, indicating relatively strong x-y mixing.

The x-z plots in fig 6b show some coupling into this plane at many momenta, but such coupling results mostly in a beat, without any instability occuring. But at the specific momentum of 10.85 GeV/c, the amplitude continues to grow without apparent limit, indicating an instability

Fig 6c shows the $x - p_x$ motion induced by the coupling (fig 6d will be fefered to below).

Fig 7a shows that this x-y coupling resonance is narrow (approx 0.1 GeV), which, relative to the energy gain per turn (approx 1 GeV), should not be a problem;

6.3 Non-linear resonance

At a tune of .25 there is a non-linear resonance in y as seen in Fig 6d. Fig 7b shows that this y instability is even narrower (.05 GeV) than the coupling resonance, and its growth rate is slow enough (amplitude increase of about 10 percent after 50 cells), that it too should not be a problem.

Resonanced in y at a tune of 0.33 were searched for and not found. No resonaces were found at tunes of 0.25 or 0.33 in the x direction.

7 Conclusion

This study has shoen that an example of a triplet non-scaling FFAG can be traced with ICOOL, using quasi-realistic fields and shows negligible non-linear effects over a 2:1 momentum range (10-20 GeV/c) and a large transverse acceptance (30 pi mm normalized). Further work can incorporate more realistic coil ends and include acceleration.

References

[1] Johnstone

[2] Trbojevic; KEK Workshop July, 2003.

[3] Meot; KEK Workshop July, 2003.

[4] ICOOL; R Fernow

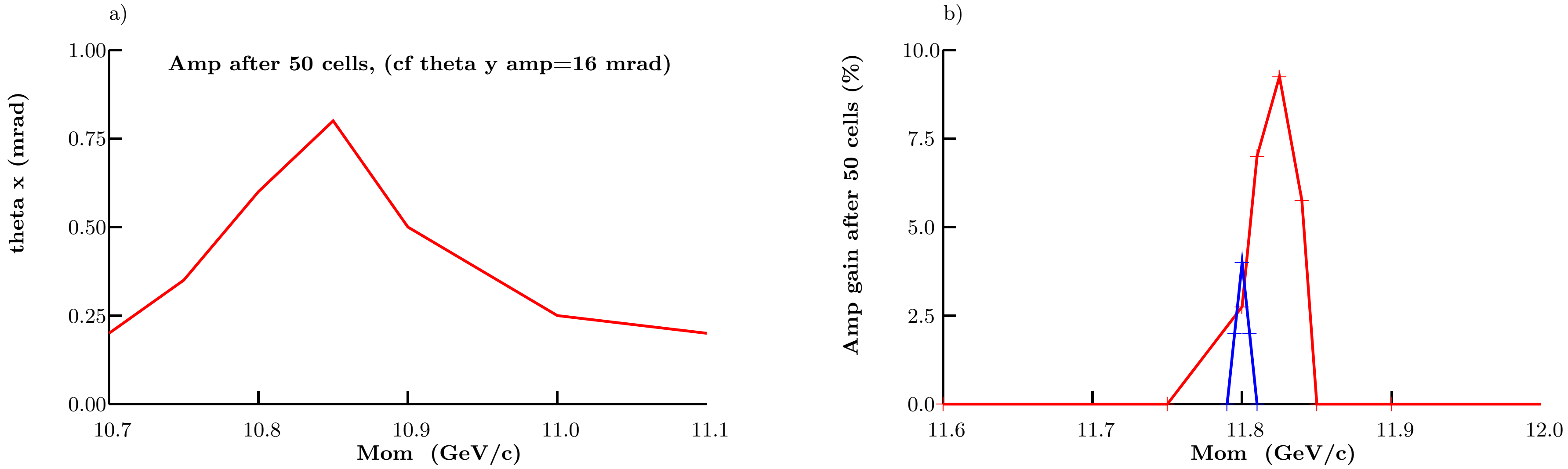

Figure 7: a) Amplitudes in x after 50 cells as function of particle momentum for 30 pi mm in y; b) Amplitude y gain after 50 cells due to 0.25 resonance in y vs particle energy, for 30 pi mm in y (red) and 30 pi mm in x & y (blue).

8 Appendix ICOOL files

```
Dejan 10-20 ffag with ends y only (demo)

$cont npart=11 nsections=50 varstep=.false. nprnt=-3 prlevel=1
ntuple=.false. rtuple=.false.  output1=.true. phasemodel=3
fsav=.false. fsavset=.false. bgen=.false.  $

 $ints ldecay=.true.  declev=1  ldedx=.true. lstrag=.true. lscatter=.true.
  delev=2 straglev=4 scatlev=4  $

 $nhs  $
 $nsc  $
 $nzh  $
 $nrh nrhist=0 $
 $nem nemit=2 pxycorr=.true. pzcorr=.true. bzfldprd=3.5 $
 1 1322
 $ncv ncovar=2 $
 1 1322

SECTION

REFP
2  15.0  0. 0. 3             !typ refp t0 grad0 mode (3=const p 4=with acc)

BEGS

!=========================================================================

CELL      !-------------------- regular cell
1
.FALSE.

BSOL                                    ! multipole field input
4. 56 15 3 0  1 1 1 1 1 1 1 1 1 0. !mode file ? order 1/r scale-factors

!----------------------------------------------------------------------


OUTPUT
SREGION                       ! define a region              DRIFT  1M
1.28 1 0.003                  ! length, 1 radial subregion, step
1 0. .1                     ! radial extent
NONE ! no associated field
0. 0. 0. 0. 0. 0. 0. 0. 0. 0. 0. 0. 0. 0. 0.
```

```
VAC ! vacuum material
CBLOCK ! cylindrical block geometry
0. 0. 0. 0. 0. 0. 0. 0. 0. 0.

OUTPUT
SREGION                       ! define a region              DRIFT  1M
.42 1 0.003                  ! length, 1 radial subregion, step
1 0. .1                     ! radial extent
NONE ! no associated field
0. 0. 0. 0. 0. 0. 0. 0. 0. 0. 0. 0. 0. 0. 0.
VAC ! vacuum material
CBLOCK ! cylindrical block geometry
0. 0. 0. 0. 0. 0. 0. 0. 0. 0.

OUTPUT
SREGION                       ! define a region              DRIFT  1M
.75 1 0.003                  ! length, 1 radial subregion, step
1 0. .1                     ! radial extent
NONE ! no associated field
0. 0. 0. 0. 0. 0. 0. 0. 0. 0. 0. 0. 0. 0. 0.
VAC ! vacuum material
CBLOCK ! cylindrical block geometry
0. 0. 0. 0. 0. 0. 0. 0. 0. 0.

OUTPUT
SREGION                       ! define a region              DRIFT  1M
.75 1 0.003                  ! length, 1 radial subregion, step
1 0. .1                     ! radial extent
NONE ! no associated field
0. 0. 0. 0. 0. 0. 0. 0. 0. 0. 0. 0. 0. 0. 0.
VAC ! vacuum material
CBLOCK ! cylindrical block geometry
0. 0. 0. 0. 0. 0. 0. 0. 0. 0.

OUTPUT
SREGION                       ! define a region              DRIFT  1M
.42 1 0.003                  ! length, 1 radial subregion, step
1 0. .1                     ! radial extent
NONE ! no associated field
0. 0. 0. 0. 0. 0. 0. 0. 0. 0. 0. 0. 0. 0. 0.
VAC ! vacuum material
CBLOCK ! cylindrical block geometry
0. 0. 0. 0. 0. 0. 0. 0. 0. 0.

OUTPUT
SREGION                       ! define a region              DRIFT  1M
```

```
1.28 1 0.003                  ! length, 1 radial subregion, step
1 0. .1                     ! radial extent
NONE ! no associated field
0. 0. 0. 0. 0. 0. 0. 0. 0. 0. 0. 0. 0. 0. 0.
VAC ! vacuum material
CBLOCK ! cylindrical block geometry
0. 0. 0. 0. 0. 0. 0. 0. 0. 0.


ENDCELL
ENDSECTION
```